2013 European Control Conference (ECC)
July 17-19, 2013, Zürich, Switzerland.

Selective Model Inversion and Adaptive Disturbance Observer For Rejection of Time-varying Vibrations On An Active Suspension

Xu Chen and Masayoshi Tomizuka

Abstract— **This paper presents an adaptive control scheme for identifying and rejecting unknown and/or time-varying narrow-band vibrations. We discuss an idea of selective model inversion (SMI) for a (possibly non-minimum phase) plant dynamics at multiple narrow frequency regions, so that vibrations can be estimated and canceled by feedback. By taking advantage of the structure of the disturbance model, we can reduce the adaptation to identify the minimum amount of parameters, achieve accurate parameter estimation under noisy environments, and flexibly reject the narrow-band disturbances with clear tuning intuitions. Evaluation of the proposed algorithm is performed via simulation and experiments on a benchmark system for active vibration control.**

I. Introduction

The rejection of multiple narrow-band disturbances is a fundamental problem in many mechanical systems that involve periodic motions. For example, the shaking mechanism in active suspensions [1], the rotating disks in hard disk drives [2], and the cooling fans for computer products [3], all generate vibrations that are composed of sinusoidal components in nature. Challenges of the problem are that we seldom have accurate knowledge of the disturbance frequencies, and that in many applications the disturbance spectra may change w.r.t. time and/or among different products. In various situations, hardware limitations or excessive re-design cost make it infeasible to reduce these disturbance by system reconstruction, and it is only possible to address the problem from the control-engineering perspective.

As narrow-band vibrations are composed of sinusoidal signal components, controllers can be customized to incorporate the disturbance structure for asymptotic disturbance rejection. This internal-model-principle [4] based perspective has been investigated in feedback control design in [1], [3], [5]–[7], among which [5], [6] used state-space designs, and [1], [3], [7] applied Youla Parameterization, a.k.a. all stabilizing controllers, with a Finite Impulse Response (FIR) adaptive Q filter. Alternatively, the disturbance frequency can be firstly estimated and then applied for controller design. This indirect-adaptive-control perspective has been considered in [8]–[10].

In this paper we discuss a new adaptive incorporation of the internal model principle for rejection of narrow-band disturbances. Different from FIR-based adaptive algorithms, we construct the design with Infinite Impulse Response (IIR) filters and inverse system models. Applying these considerations we are able to obtain a structured controller parameterization that requires the minimum amount of adaptation parameters. An additional consideration is that adaptation on IIR structures enables the usage of adaptation algorithms that use the parallel predictor, which is essential for accurate parameter convergence under noisy environments [11]. Finally, with the inverse-model based design, the internal signals in the proposed algorithm have clear physical meanings. This helps the tuning of the algorithm, particularly in industrial applications. The controller structure is an extension of the idea in [2]. The main part of this paper, i.e., the design of inverse models, the derivation of the cascaded IIR filters, and the adaptation algorithm for time-varying disturbance rejection are, however, all newly developed. An additional contribution is the application to a new class of systems that has characteristics quite different from the hard disk drive in [2].

The solid line in Fig. 1 shows the frequency response of the active suspension system on which our algorithm is evaluated. This system serves as a benchmark on adaptive regulation in [12]. It has a group of resonant and anti-resonant modes, especially at around 50 and 100 Hz. Additionally, the system is open-loop stable but has multiple lightly damped zeros at mid frequencies and nonminimum-phase zeros at high frequencies. These characteristics place additional challenges not just for adaptive disturbance rejection, but also for general feedback control [13].

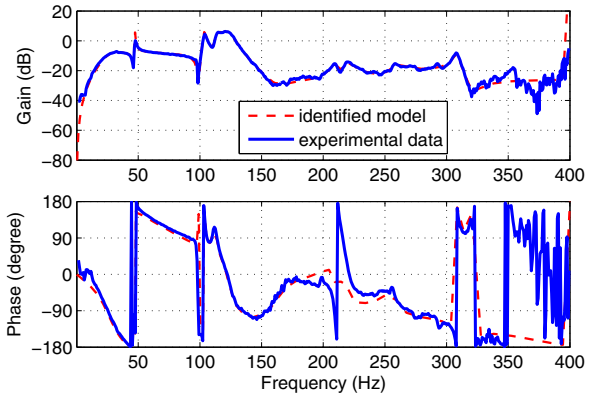

Fig. 1. Frequency response of the plant

X. Chen and M. Tomizuka are with Department of Mechanical Engineering, University of California, Berkeley, CA, 94720, USA (email: maxchen@me.berkeley.edu; tomizuka@me.berkeley.edu)

II. Selective Model Inversion

Fig. 2 shows the proposed control scheme. We have the following relevant signals and transfer functions:

- $P(z^{-1})$ and $\hat{P}(z^{-1})$: the plant under control and its identified model;
- $C(z^{-1})$: a baseline controller designed to provide a robustly stable closed loop;
- $d(k)$ and $\hat{d}(k)$: the actual (unmeasurable) disturbance and its online estimate (note that $\hat{d}(k) = P(q^{-1})u(k) + d(k) - \hat{P}(q^{-1})u(k) \approx d(k)$, where q^{-1} is the one-step-delay operator[1]);
- $y(k)$: measured residual error;
- Parameter adaptation algorithm: provides online information of the characteristics of $\hat{d}(k)$;
- $c(k)$: the compensation signal to asymptotically reject the narrow-band disturbance in $d(k)$;
- $P_m^{-1}(z^{-1})$ and z^{-m}: these are constructed such that: (i) $P_m(z^{-1})$ has a relative degree of zero (and hence $P_m^{-1}(z^{-1})$ is realizable); (ii) $P_m^{-1}(z^{-1})$ is stable; and (iii) within the frequency range of the possible disturbances, $P(z^{-1})\big|_{z=e^{j\omega}} \approx z^{-m}P_m(z^{-1})\big|_{z=e^{j\omega}}$, namely, $P_m^{-1}(z^{-1})$ is a nominal inverse (without delays) model of $P(z^{-1})$.

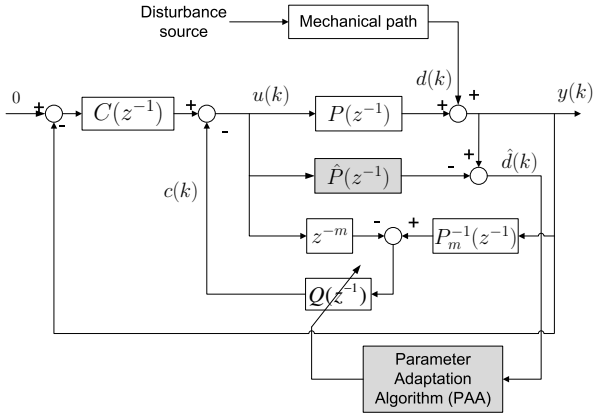

Fig. 2. Structure of the proposed control scheme

The intuition of the block-diagram construction is to design the disturbance observer (estimator) to generate the compensation signal $c(k)$ that approximates $P^{-1}(q^{-1})d(k)$ if $d(k)$ contains just narrow-band vibrations. This forms the idea of a narrow-band disturbance observer [2]. To see this, ignore first the shaded blocks (about parameter adaptation) in Fig. 2, then the control signal $u(k)$ flows through two paths to reach the summing junction before $Q(z^{-1})$: one from the plant $P(z^{-1})$ to the inverse $P_m^{-1}(z^{-1})$, and the other through z^{-m}. Hence the effect of $u(k)$ gets canceled at the entrance of $Q(z^{-1})$, and only the filtered disturbance $P_m^{-1}(q^{-1})d(k)$ enters the filter $Q(z^{-1})$. To develop the structure of $Q(z^{-1})$, we can derive the sensitivity function, namely, the transfer function from $d(k)$ to $y(k)$:

$$S(z^{-1}) = G_{d2y}(z^{-1}) = \left(1 - z^{-m}Q(z^{-1})\right)/X(z^{-1}) \quad (1)$$

$$X(z^{-1}) \triangleq 1 + P(z^{-1})C(z^{-1}) + Q(z^{-1})(P_m^{-1}(z^{-1})P(z^{-1}) - z^{-m}) \quad (2)$$

From the frequency-response perspective, if $P(e^{-j\omega}) = e^{-jm\omega}P_m(e^{-j\omega})$ in (1) and (2), then the last term in $X(e^{-j\omega})$ vanishes and

$$S(e^{-j\omega}) = \left(1 - e^{-jm\omega}Q(e^{-j\omega})\right)/\left(1 + P(e^{-j\omega})C(e^{-j\omega})\right). \quad (3)$$

If we design a Q-filter, $Q(z^{-1})$, as shown in Fig. 3, then $1 - e^{-mj\omega}Q(e^{-j\omega})$, and thus $G_{d2y}(e^{-j\omega})$ in (1), will become zero at the center frequencies of $Q(z^{-1})$ (in this example, 60 Hz and 90 Hz), namely, disturbances occurring at these frequencies will be strongly attenuated. Assume first that vibrations occur exactly at 60 Hz and 90 Hz. $Q(z^{-1})$ will filter out all other frequency components such that its output $c(k)$ consists of signals only at the disturbance frequencies.

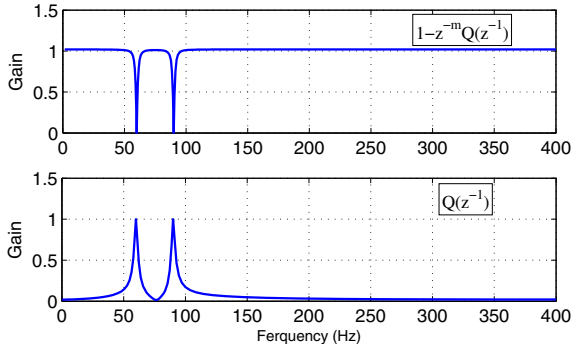

Fig. 3. Frequency response of a Q-filter example

We remark that the shape of $Q(z^{-1})$ in Fig. 3 is central in the proposed design scheme. Uncertainties exist in $P(z^{-1})$ no matter how accurate $P_m(z^{-1})$ is constructed (based on modeling or system identification). It is not practical (and is even dangerous) to invert $P(z^{-1})$ over the entire frequency region. Keeping the magnitude of $Q(z^{-1})$ small except at the interested disturbance frequencies forms a selective (i.e., local/selected) model inverse (SMI) of the plant dynamics, such that errors due to model mismatches do not pass through $Q(z^{-1})$ and equation (3) remains a valid approximation of (1). In this way, the system stability is easily preserved as $1/(1 + P(z^{-1})C(z^{-1}))$ is the sensitivity function of the baseline system (and hence stable). A stable $Q(z^{-1})$ in this case will assure the stability of $S(z^{-1}) \approx (1 - z^{-m}Q(z^{-1}))/(1 + P(z^{-1})C(z^{-1}))$. Of course, an assumption here is that good model information can be obtained at the disturbance frequencies. If the system already has large uncertainties at the disturbance frequencies, it is best not to apply large control effort there in the first place.

[1]In this paper, $P(z^{-1})$, $P(q^{-1})$, and $P(e^{-j\omega})$ are used to denote respectively the transfer function, the pulse transfer function, and the frequency response of $P(z^{-1})$ at ω.

III. Design of The Inverse Dynamics

In the aforementioned analysis we have assumed $P_m^{-1}(z^{-1})$ to be stable. It is well known that nonminimum-phase zeros in $P(z^{-1})$ not only make $P^{-1}(z^{-1})$ unstable but also cause control limitations (see, e.g., [13]). The benchmark system has multiple of such zeros. We discuss next an H_∞ treatment of the nonminimum-phase plant when designing $P_m^{-1}(z^{-1})$.

With the input-output data, standard system identification can be performed to obtain $P(z^{-1})$ (we use the subspace system identification technique [14]). Let $\mathbf{S}$ denote the set of all stable discrete-time rational transfer functions, and recall the ideal situation where $P(z^{-1}) = z^{-m}P_m(z^{-1})$. We search among $\mathbf{S}$ to find $M(z^{-1}) = P_m^{-1}(z^{-1})$ such that the following are satisfied:

(i) model matching: to minimize the cost function $\|W_1(z^{-1})\left(M(z^{-1})P(z^{-1}) - z^{-m}\right)\|_\infty$, namely, we minimize the maximum magnitude of the model mismatch $M(z^{-1})P(z^{-1}) - z^{-m}$, weighted by $W_1(z^{-1})$. The ideal solution, if $P^{-1}(z^{-1})$ is stable, is simply $M(z^{-1}) = z^{-m}P^{-1}(z^{-1})$. The weighting function $W_1(z^{-1})$ determines the region where we would like to have good model accuracy.

(ii) gain constraint: as the inverse is used for processing the measured output signal in Fig. 2, we should be careful not to amplify the noises in $y(k)$. Consider the problem of $\min\|W_2(z^{-1})M(z^{-1})P(z^{-1})\|_\infty$, where the magnitude of $M(z^{-1})P(z^{-1})$ is scaled by the weight $W_2(z^{-1})$. If $W_2(z^{-1}) = 1$, the optimal solution for this part alone would be $M(z^{-1}) = 0$, i.e., $M(z^{-1})$ will not amplify any of its input components. To make full use of this gain constraint, we combine it with the previous discussion to form:

$$\min_{K(z^{-1})\in\mathbf{S}} \left\| \begin{bmatrix} W_1(z^{-1})\left(M(z^{-1})P(z^{-1}) - z^{-m}\right) \\ W_2(z^{-1})M(z^{-1})P(z^{-1}) \end{bmatrix} \right\|_\infty . \quad (4)$$

The optimization in (4) finds the optimal inverse that preserves accurate model information in the frequency region specified by $W_1(z^{-1})$, and in the meantime penalizes excessive high gains of $M(z^{-1})$ at frequencies where $W_2(z^{-1})$ has high magnitudes. Typically $W_1(z^{-1})$ is a low-pass filter and $W_2(z^{-1})$ is a high-pass filter.

By the formulation of the problem, (4) falls into the framework of H_∞ control, and can be efficiently solved in the robust control toolbox in MATLAB. Actually, the dashed line in Fig. 1 is the $z^{-m}P_m(z^{-1})$ obtained from the proposed H_∞ problem. We can see that the optimal solution matches well with the actual plant dynamics, and moreover, $P_m^{-1}(z^{-1})$ is stable although $P(z^{-1})$ is nonminimum-phase.

IV. Disturbance-Observer Design

With the inverse and other filters specified in Fig. 3, it remains to design $Q(z^{-1})$, which is the heart for SMI and the disturbance observer. For narrow-band vibrations caused by sinusoidal excitations, there exist configurations that can achieve optimal disturbance rejection.

Recall (1). To regulate $y(k) = S(q^{-1})d(k)$ to zero, it suffices to design $Q(z^{-1})$ such that at the steady state

$$\left(1 - q^{-m}Q(q^{-1})\right)d(k) = 0. \quad (5)$$

We propose an IIR structure $Q(z^{-1}) = B_Q(z^{-1})/A_Q(z^{-1})$. For vibrations satisfying $d(k) = \sum_{i=1}^{n} C_i \sin(\omega_i k + \psi_i)$, it can be verified that $\left(1 - 2\cos(\omega_i)q^{-1} + q^{-2}\right)C_i \sin(\omega_i k + \psi_i) = 0$. Define

$$A(z^{-1}) \triangleq \prod_{i=1}^{n} (1 - 2\cos(\omega_i)z^{-1} + z^{-2}), \quad (6)$$

then (5) is achieved if

$$1 - z^{-m}Q(z^{-1}) = K(z^{-1})\frac{A(z^{-1})}{A_Q(z^{-1})}. \quad (7)$$

To get a $1 - z^{-m}Q(z^{-1})$ that has a magnitude response similar to that in Fig. 3, $A(z^{-1})/A_Q(z^{-1})$ should have a notch-filter structure. A natural choice is to damp the roots of $A(z^{-1})$ by a scalar $\alpha \in (0,1)$ and let $A_Q(z^{-1}) \triangleq \prod_{i=1}^{n}\left(1 - 2\alpha\cos(\omega_i)z^{-1} + \alpha^2 z^{-2}\right)$, i.e., $A_Q(z^{-1}) = A(\alpha z^{-1})$. This will later benefit the parameter adaptation algorithm. To see this, expanding the product in (6) yields

$$A(z^{-1}) = 1 + a_1 z^{-1} + \cdots + a_n z^{-n} + \cdots + a_1 z^{-2n+1} + z^{-2n}, \quad (8)$$

where we have mapped the parameters $\{\omega_i\}_1^n$ in (6) to $\{a_i\}_1^n$, and the new coefficient vector $\{1, a_1, \ldots, a_n, \ldots, a_1, 1\}$ has a mirror symmetric form by the construction of $A(z^{-1})$. Replacing every z^{-1} with αz^{-1}, we obtain $A_Q(z^{-1}) = A(\alpha z^{-1})$, which is also linear in $\{a_i\}_1^n$. Therefore only these n parameters need to be later identified. This is the minimum possible number for n unknown narrow-band signals.

The filter $K(z^{-1})$ is necessary to make the solution causal for a general m. Without $K(z^{-1})$, (7) indicates that $Q(z^{-1}) = z^m(A_Q(z^{-1}) - A(z^{-1}))/A_Q(z^{-1})$, where the non-realizable z^m is non-trivial to cancel. A design guide for $K(z^{-1})$ is that it should not introduce serious magnitude distortion to the achieved notch shape of $A(z^{-1})/A_Q(z^{-1}) = A(z^{-1})/A(\alpha z^{-1})$ in (7). This way we can control the noise amplification in (5) when $d(k)$ contains other disturbances not modeled by (6). We discuss next choices of $K(z^{-1})$ for different values of m.

A. The case for $m = 0$

For the simplest case $m = 0$, a scalar value $K(z^{-1}) = k_0$ provides a realizable solution to (7). Recalling $Q(z^{-1}) = B_Q(z^{-1})/A_Q(z^{-1}) = B_Q(z^{-1})/A(\alpha z^{-1})$ and (8), we can reduce (7) to $A(\alpha z^{-1}) - B_Q(z^{-1}) = k_0 A(z^{-1})$, which yields

$$\begin{aligned} B_Q(z^{-1}) = (1 - k_0) + (\alpha - k_0)a_1 z^{-1} + \cdots + (\alpha^n - k_0)a_n z^{-n} \\ + \cdots + (\alpha^{2n-1} - k_0)a_1 z^{-2n+1} + (\alpha^{2n} - k_0)z^{-2n}. \end{aligned} \quad (9)$$

It can be shown [15] that $k_0 = \alpha^n$ leads to the common factor $1 - \alpha z^{-2}$ in $B_Q(z^{-1})$, which places two symmetric

zeros to $Q(z^{-1})$ at $\pm\sqrt{\alpha}$. This provides balanced magnitude response for $Q(z^{-1})$ at low- and high-frequencies.

B. The case for $m = 1$

Applying analogous analysis as in Section IV-A, we reduce (7) to $A(\alpha z^{-1}) - z^{-1}B_Q(z^{-1}) = k_0 A(z^{-1})$, the solution of which is $B_Q(z^{-1}) = (1-k_0)z + (\alpha - k_0)a_1 + \cdots + (\alpha^n - k_0)a_n z^{-n+1} + \cdots + (\alpha^{2n-1} - k_0)a_1 z^{-2n+2} + (\alpha^{2n} - k_0)z^{-2n+1}$.

To let the term $(1-k_0)z$ vanish for realizability, we require $k_0 = 1$, which gives

$$B_Q(z^{-1}) = \sum_{i=1}^{2n} (\alpha^i - 1)a_i z^{-i+1};\ a_i = a_{2n-i},\ a_{2n} = 1. \tag{10}$$

As an example, when $n = 1$, (6), (8) and (10) yield $a_1 = -2\cos\omega_1$ and

$$Q(z^{-1}) = \frac{(1-\alpha)\left(2\cos\omega_1 - (1+\alpha)z^{-1}\right)}{1 - 2\alpha\cos\omega_1 z^{-1} + \alpha^2 z^{-2}}.$$

Using the identity $2\cos(\omega_1) = e^{j\omega_1} + e^{-j\omega_1}$, we can obtain that $Q(e^{-j\omega_1}) = e^{j\omega_1}$. Thus, $Q(z^{-1})$ provides exactly one-step advance to counteract the one-step delay in $z^{-1}Q(z^{-1})$ at the center frequency ω_1, hence the zero magnitude response of $1 - z^{-1}Q(z^{-1})$ at ω_1.

C. The case for an arbitrary m

For $m > 1$, assigning $K(z^{-1}) = k_0$ no longer gives a realizable solution. Consider the following IIR design

$$K(z^{-1}) = \sum_{i=0}^{N} k_i \left[\frac{A(z^{-1})}{A(\alpha z^{-1})}\right]^i,\ k_i \in \mathcal{R}. \tag{11}$$

Namely, $K(z^{-1})$ is chosen as a combination of $N(\geq 0)$ filters that influence only the local loop shape (recall that $A(z^{-1})/A(\alpha z^{-1})$ is a notch filter). Take the example of $m = 2$. When $N = 1$,[2] solving (7) gives

$$Q(z^{-1}) = z^2\left(1 - k_0\frac{A(z^{-1})}{A(\alpha z^{-1})} - k_1\frac{A(z^{-1})^2}{A(\alpha z^{-1})^2}\right). \tag{12}$$

Partitioning, we obtain

$$Q(z^{-1}) \triangleq z^2\left(1 - \rho_1\frac{A(z^{-1})}{A(\alpha z^{-1})}\right)\left(1 - \rho_2\frac{A(z^{-1})}{A(\alpha z^{-1})}\right). \tag{13}$$

The numerator of $Q(z^{-1})$ is given by $B_Q(z^{-1}) = z^2(A(\alpha z^{-1}) - \rho_1 A(z^{-1}))(A(\alpha z^{-1}) - \rho_2 A(z^{-1}))$. Recalling (8) we have $A(\alpha z^{-1}) - \rho_i A(z^{-1}) = (1-\rho_i) + (\alpha - \rho_i)a_1 z^{-1} + \cdots + (\alpha^{2n} - \rho_i)z^{-2n}$. To make the z^2 term vanish in $B_Q(z^{-1})$ for realizability of $Q(z^{-1})$, we must have $1 - \rho_i = 0$ for $i = 1, 2$, yielding $k_0 = 2$, $k_1 = -1$ in (12). With these solved ρ_i and k_i, after simplification, (13) and (11) become

$$Q(z^{-1}) = \left[\frac{\sum_{i=1}^{2n}(\alpha^i - 1)a_i z^{-i+1}}{A(\alpha z^{-1})}\right]^2;\ a_i = a_{2n-i},\ a_{2n} = 1 \tag{14}$$

$$K(z^{-1}) = 2 - \frac{A(z^{-1})}{A(\alpha z^{-1})}. \tag{15}$$

[2]If $N = 0$, the problem is unsolvable since $K(z^{-1})$ is a scalar again.

For a general integer m, analogous analysis gives that

$$Q(z^{-1}) = \left[\frac{\sum_{i=1}^{2n}(\alpha^i - 1)a_i z^{-i+1}}{A(\alpha z^{-1})}\right]^m \tag{16}$$

$$1 - z^{-m}Q(z^{-1}) = 1 - \left(1 - \frac{A(z^{-1})}{A(\alpha z^{-1})}\right)^m \tag{17}$$

$$= \frac{A(z^{-1})}{A(\alpha z^{-1})}\sum_{i=1}^{m}\binom{m}{i}\left[-\frac{A(z^{-1})}{A(\alpha z^{-1})}\right]^{i-1} \tag{18}$$

It can be observed that the general result obtained here is essentially a cascaded version of the developed $Q(z^{-1})$ in Section IV-B. For the sake of clarity, we denote now the Q filter for $m = 0$ and $m = 1$ respectively as $Q_0(z^{-1})$ and $Q_1(z^{-1})$. As has been discussed at the end of Section IV-B, $Q_1(z^{-1})$ provides 1 step phase advance to address the term z^{-1} in $1 - z^{-1}Q_1(z^{-1})$. For a general m, we see that the cascaded $Q(z^{-1}) = \left[Q_1(z^{-1})\right]^m$ in (16) works the same way due to the factorization $1 - z^{-m}Q(z^{-1}) = 1 - (z^{-1}Q_1(z^{-1}))^m$, i.e., each $Q_1(z^{-1})$ block compensates one z^{-1} term, to achieve $1 - e^{-jm\omega}Q(e^{-j\omega}) = 0$ when ω belongs to the set of disturbance frequencies $\{\omega_i\}_1^n$. Recall from Fig. 3, that $Q(z^{-1})$ is a special type of bandpass filter. Cascading multiple $Q_1(z^{-1})$ together not only provides the compensation for z^{-m}, but also provides enhanced filter shape. If needed, we can additionally cascade one or multiple blocks of $Q_0(z^{-1})$ to $Q(z^{-1})$, which will further reduce the filter magnitude outside the passband, without losing the disturbance-rejection property at the center frequencies of $Q(z^{-1})$.

V. Parameter Adaptation

This section discusses the online adaptation of the parameters $\{a_i\}_{i=1}^n$ in $Q(z^{-1})$ when the disturbance characteristics is not known *a priori*. Recall from Fig. 2, that

$$y(k) = G_{d2y}(q^{-1})d(k) = S(q^{-1})d(k) \approx \frac{1 - q^{-m}Q(q^{-1})}{1 + P(q^{-1})C(q^{-1})}d(k).$$

The beginning of Section II has discussed the obtaining of $\hat{d}(k) \approx d(k)$. Letting $w_1(k) \triangleq \hat{d}(k)/(1 + P(q^{-1})C(q^{-1}))$ and recalling the solution of $1 - q^{-m}Q(q^{-1})$ in (18), we get

$$y(k) \approx \left\{\sum_{i=1}^{m}\binom{m}{i}\left[-\frac{A(q^{-1})}{A(\alpha q^{-1})}\right]^{i-1}\right\}\frac{A(q^{-1})}{A(\alpha q^{-1})}w_1(k)$$

For vibration rejection, $y(k)$ will converge to zero if $A(q^{-1})/A(\alpha q^{-1})w_1(k)$ is asymptotically zero. We will use $w_2(k) \triangleq A(q^{-1})/A(\alpha q^{-1})w_1(k)$ as an adaptation model,[3] which is linear w.r.t. the unknown coefficients $\theta \triangleq [a_1, a_2, \ldots, a_n]^T$. The structure is a special (and simplified) one for adaptive control due to the close relationship between $A(q^{-1})$ and $A(\alpha q^{-1})$. The full parameter adaptation algorithm (PAA) is provided in [15]. Limited by space, we focus on the application of the PAA

[3]Additional filtering can be applied on w_1 to improve the signal-to-noise ratio. See, e.g., [10].

for identifying different time-varying vibrations. Recall that the general adaptation formula has the structure:

$$\hat{\theta}(k+1) = \hat{\theta}(k) + [\text{Adaptation gain} \times \text{Error}]$$

$$F(k+1) = \frac{1}{\lambda(k)}\left[F(k) - \frac{F(k)\phi(k)\phi(k)^T F(k)}{\lambda(k) + \phi(k)^T F(k)\phi(k)}\right]$$

where $F(k)$ is the adaptation gain and the forgetting factor $\lambda(k)$ determines how much information is used for adaptation. It is well-known that altering the forgetting factor is the key for time-varying parameter adaptationWe suggest the following tuning rules:

(i) rapid initial convergence: initialize $\lambda(k)$ to be exponentially increasing from λ_0 to 1 in the first several samples, where λ_0 can be taken to be between $[0.92, 1)$

(ii) adjustment for sudden parameter change: when the prediction error encounters a sudden increase, indicating a change of disturbance characteristics, reduce $\lambda(k)$ to a small value $\underline{\lambda}$ (e.g. 0.92 in the benchmark), and then increase it back to its steady-state value $\overline{\lambda}$ (usually close to 1), using the formula $\lambda(k) = \overline{\lambda} - \lambda_{\text{rate}}(\overline{\lambda} - \lambda(k-1))$, with λ_{rate} preferably in the range $(0.9, 0.995)$.

(iii) adjustment for continuously changing parameters: in this case, keep $\lambda(k)$ strictly smaller than one, using e.g., a constant $\lambda(k)(< 1)$.

VI. Simulation and Experimental Results

We apply in this section the proposed scheme to the benchmark problem. In this system, the plant delay $m = 2$ in the modeling of $P(z^{-1})\big|_{z=e^{j\omega}} \approx z^{-m}P_m(z^{-1})\big|_{z=e^{j\omega}}$. Hence two $Q_1(z^{-1})$ blocks are needed in (16). Vibrations occur in the middle frequency region between 50 Hz and 95 Hz. There are also other noises at low and high frequencies. To enhance the bandpass property, we cascaded one additional $Q_0(z^{-1})$ block designed in Section IV-A to $Q(z^{-1})$, and prefiltered the input to the PAA (denoted as $w_1(k)$ in Section V) by a bandpass filter (passband: 50–95 Hz) to remove the bias and other high-frequency noises in the estimated disturbance.

In the first stage of evaluation (denoted as level-one test), the system is subjected to a single-frequency vibration. Three cases are studied: the first with a constant unknown frequency, the second with a sudden frequency change at specific time instances, and the third with a chirp disturbance.

Fig. 4 show the output spectra with and without the proposed scheme. We can observe first, that the simulation and the experimental results match well, and that in both cases the strong vibrations have been greatly attenuated, while the spectra at other frequencies are nearly identical to that without compensation. Fig. 5 shows the time trace (experimental result) of the residual errors when the disturbance frequency has abrupt changes. In the presence of various frequency jumps, the algorithm still provides rapid and strong vibration compensation. Comparing the data at 2 sec and 7 sec, we see the steady-state residual errors have been reduced to the baseline case where no narrow-band disturbance is present.

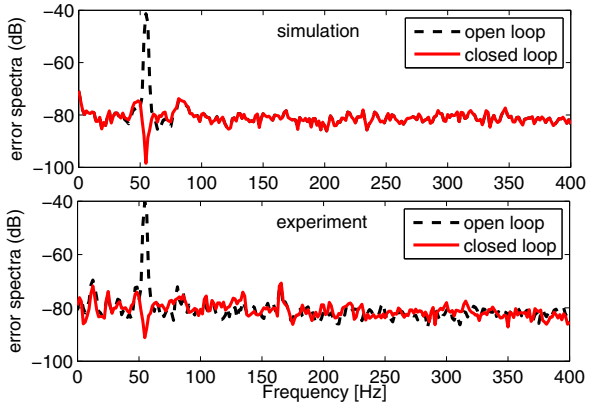

Fig. 4. Rejection of a 55 Hz vibration

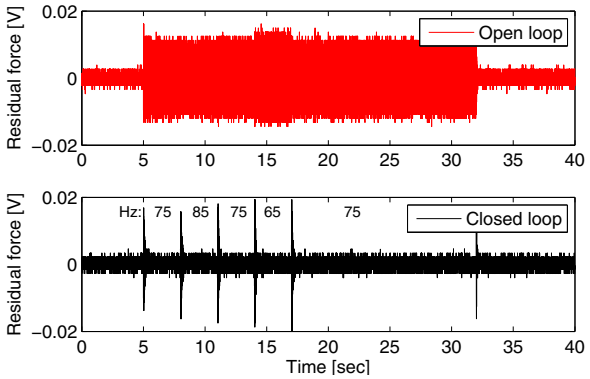

Fig. 5. Experimental results of rejecting a vibration with frequency jumps (frequency values indicated in the bottom subplot)

Fig. 6 shows the compensation results when the disturbance frequency experienced a chirp-type evolution between 50 Hz and 95 Hz. Fig. 7 shows the identified frequency (computed offline from $a_1 = -2\cos\omega_1$, where a_1 is updated online). Under such time-varying frequencies, we see the proposed algorithm maintains its effectiveness of compensating the disturbance.

Figs. 8 to 11 show the experimental results of rejecting two and three narrow-band disturbances. Again, disturbances with different time-domain characteristics are tested as shown in Figs. 8 and 10. From Figs. 9 and 11, the strong spectral peaks in the specified frequency region [50–95] Hz are all strongly attenuated. There are several peaks outside the 50–95 Hz window. They are not amplified in the closed-loop response (some of them are actually attenuated). Indeed, the proposed algorithm has the property of maintaining very small amplification of other disturbances (see also Fig. 4), due to the frequency-domain design criterion in Fig. 3. The benchmark has set up several evaluation quantities about performance, robustness, and complexity. The proposed algorithm achieved 100% in the benchmark

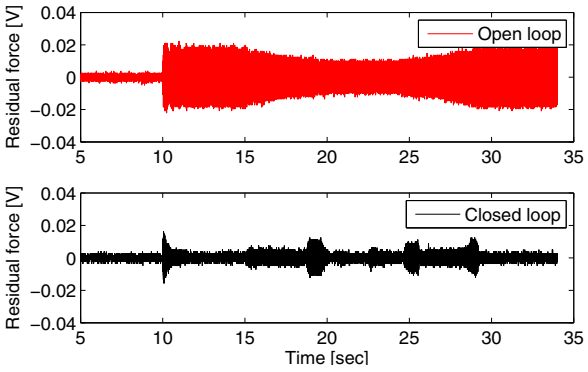

Fig. 6. Rejection of a narrow-band disturbance with a chirp frequency (experimental result)

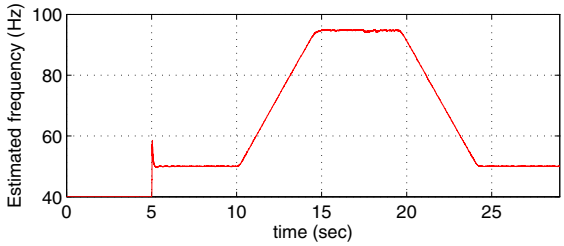

Fig. 7. Identified frequency for the case of Fig. 6

specification index for transient performance; 100%, 100%, and 99.78% respectively in steady-state simulation performance; and ranked 1, 3, and 2, respectively in experimental results. The recorded task execution time is also moderate. Detailed summaries and comparison are provided in [16].

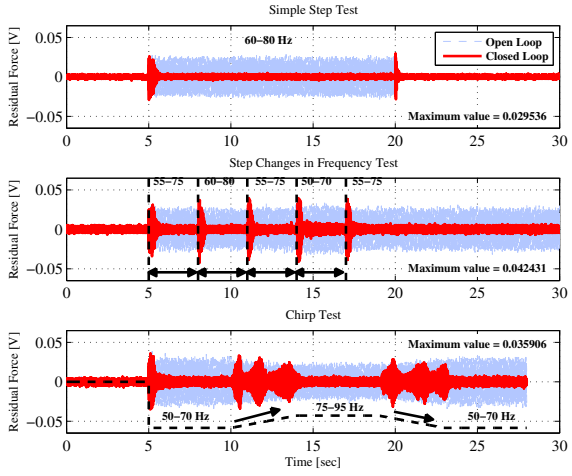

Fig. 8. Time-domain level-2 experimental results

VII. Conclusions

An adaptive control scheme has been introduced for multiple narrow-band disturbance rejection. Applications to a benchmark on active suspension showed that the proposed algorithm significantly attenuated the disturbance under various time-varying characteristics.

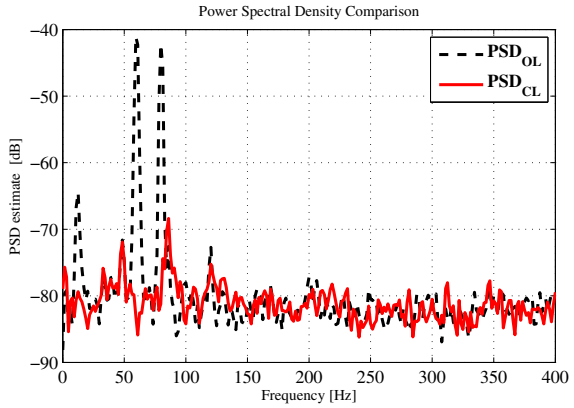

Fig. 9. Frequency-domain level-2 experimental results

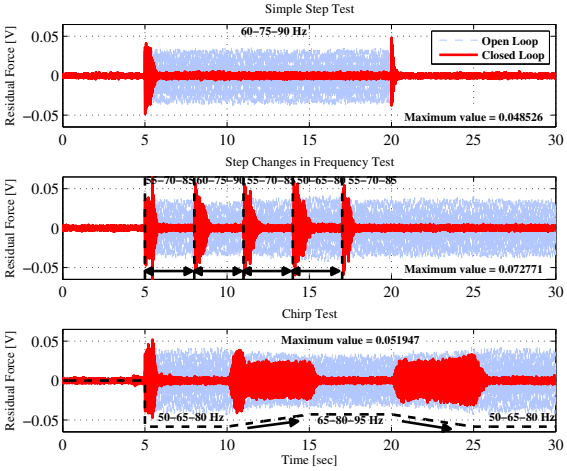

Fig. 10. Time-domain level-3 experimental results

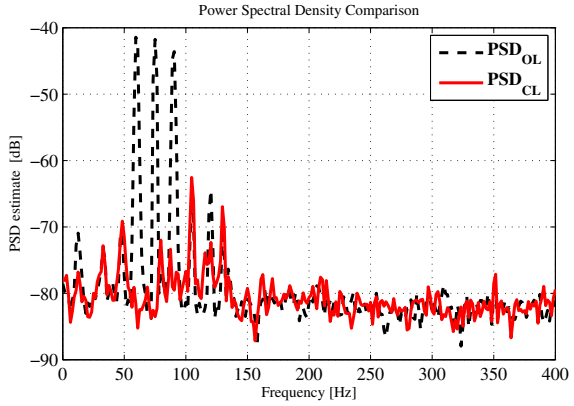

Fig. 11. Frequency-domain level-3 experimental results

VIII. Acknowledgment

The authors thank Abraham Castellanos Silva for his help on obtaining the experimental results.

References

[1] I.-D. Landau, M. Alma, J.-J. Martinez, and G. Buche, "Adaptive suppression of multiple time-varying unknown vibrations using an inertial actuator," *IEEE Trans. Control Syst. Technol.*, vol. 19, no. 6, pp. 1327–1338, 2011.

[2] X. Chen and M. Tomizuka, "A minimum parameter adaptive approach for rejecting multiple narrow-band disturbances with application to hard disk drives," *IEEE Trans. Control Syst. Technol.*, vol. 20, pp. 408 – 415, March 2012.

[3] C. Kinney, R. de Callafon, E. Dunens, R. Bargerhuff, and C. Bash, "Optimal periodic disturbance reduction for active noise cancelation," *J. of Sound and Vib.*, vol. 305, no. 1-2, pp. 22–33, Aug. 2007.

[4] B. Francis and W. Wonham, "The internal model principle of control theory," *Automatica*, vol. 12, no. 5, pp. 457–465, 1976.

[5] Q. Zhang and L. Brown, "Noise analysis of an algorithm for uncertain frequency identification," *IEEE Trans. Autom. Control*, vol. 51, no. 1, pp. 103–110, 2006.

[6] W. Kim, H. Kim, C. Chung, and M. Tomizuka, "Adaptive output regulation for the rejection of a periodic disturbance with an unknown frequency," *IEEE Trans. Control Syst. Technol.*, vol. 19, no. 5, pp. 1296–1304, 2011.

[7] F. Ben-Amara, P. T. Kabamba, and a. G. Ulsoy, "Adaptive sinusoidal disturbance rejection in linear discrete-time systems–part I: Theory," *ASME J. Dyn. Syst., Meas., Control*, vol. 121, no. 4, pp. 648–654, 1999.

[8] Y. Kim, C. Kang, and M. Tomizuka, "Adaptive and optimal rejection of non-repeatable disturbance in hard disk drives," in *Proc. 2005 IEEE/ASME International Conf. on Advanced Intelligent Mechatronics*, vol. 1, 2005, pp. 1–6.

[9] Q. Jia and Z. Wang, "A new adaptive method for identification of multiple unknown disturbance frequencies in hdds," *IEEE Trans. Magn.*, vol. 44, no. 11 Part 2, pp. 3746–3749, 2008.

[10] X. Chen and M. Tomizuka, "An indirect adaptive approach to reject multiple narrow-band disturbances in hard disk drives," in *Proc. 2010 IFAC Symp. on Mechatron. Syst., Sept. 13-15, 2010 Cambridge, Massachusetts, USA*, 2010, pp. 44–49.

[11] L. Ljung, *System Identification: Theory for the User*, 2nd ed. Prentice Hall PTR, 1999.

[12] I. D. Landau, T.-B. Airimitoaie, A. C. Silva, and G. Buche, "An active vibration control system as a benchmark on adaptive regulation," in *2013 European Control Conf., July 17-19 (to appear)*.

[13] S. Skogestad and I. Postlethwaite, *Multivariable Feedback Control: Analysis and Design*, 2nd ed. Wiley Chichester, UK, 2005.

[14] P. Overschee, B. Moor, D. Hensher, J. Rose, W. Greene, K. Train, W. Greene, E. Krause, J. Gere, and R. Hibbeler, *Subspace Identification for the Linear Systems: Theory–Implementation*. Boston: Kluwer AcademicPublishers, 1996.

[15] X. Chen and M. Tomizuka, "Selective model inversion and adaptive disturbance observer for rejection of time-varying vibrations on an active-suspension benchmark," in *European Journal of Control (to appear)*.

[16] I.-D. Landau, A. C. Silva, T.-B. Airimitoaie, G. Buche, and M. Noe, "Benchmark on adaptive regulation – rejection of unknown/time-varying multiple narrow band disturbances," in *European Journal Control, 2013 (to appear)*.